PAPER

Hypercomplex Polar Fourier Analysis for Image Representation

Zhuo YANG[†a)], *Nonmember and* **Sei-ichiro KAMATA**[†b)], *Member*

SUMMARY Fourier transform is a significant tool in image processing and pattern recognition. By introducing a hypercomplex number, hypercomplex Fourier transform treats a signal as a vector field and generalizes the conventional Fourier transform. Inspired from that, hypercomplex polar Fourier analysis that extends conventional polar Fourier analysis is proposed in this paper. The proposed method can handle signals represented by hypercomplex numbers as color images. The hypercomplex polar Fourier analysis is reversible that means it can be used to reconstruct image. The hypercomplex polar Fourier descriptor has rotation invariance property that can be used for feature extraction. Due to the noncommutative property of quaternion multiplication, both left-side and right-side hypercomplex polar Fourier analysis are discussed and their relationships are also established in this paper. The experimental results on image reconstruction, rotation invariance, color plate test and image retrieval are given to illustrate the usefulness of the proposed method as an image analysis tool.

key words: *hypercomplex polar Fourier analysis, hypercomplex polar Fourier descriptor, rotation invariance, image representation*

1. Introduction

Fourier transforms have been widely used in image processing, pattern recognition and other engineering fields [1]. By representing image as hypercomplex numbers, especially the quaternions discovered by Hamilton [2], Hypercomplex Fourier transform is proposed as generalization of quaternion Fourier transform for color image processing [3], [4]. Efficient algorithm for quaternion Fourier transform is discussed by using two complex two dimensional Fourier transforms [5]. The relationship between right-side quaternion Fourier transform and left-side quaternion Fourier transform is established [6]. Fourier transform for biquaternion-valued signals and its fast algorithm that based on four complex two dimensional Fourier transforms is proposed [7]. Based on hypercomplex Fourier transform, effective algorithms for motion estimation in color image sequences are studied [8]. Quaternion Fourier-Mellin moments are proposed as rotation and scale invariant feature by using quaternion Fourier transform [9]. Rather than separating a color image into several scalar images, Hypercomplex Fourier transform treats it as vector field and acts as holistic manner.

By applying Fourier analysis to polar and spherical coordinates, Polar Fourier Descriptor (PFD) and Spherical Fourier Descriptor (SFD) are proposed as rotation invariant descriptors for analyzing 2D and 3D images, and they demonstrated superior performances comparable with other methods [10]. PFD introduces Foureir-Bessel series that is mainly used on physics-related applications [11], [12] to image analysis. Different from other Fourier descriptors that have been used for shape description [13] and image retrieval [14], [15], PFD and SFD hold orthogonal property and can characterize the image using a set of mutually independent functions. Unfortunately, the high computational complexity is the constraint for widely use because the coefficients computation involves many Bessel function, associated Legendre polynomials [16] and trigonometric computations. Our previous work [17] studied fast algorithms to reduce the computational complexity.

This paper focuses on hypercomplex polar Fourier analysis and its properties. Inspired by the hypercomplex Fourier transforms, we establish theory for polar Fourier analysis with hypercomplex numbers representation. The proposed transform is reversible that means can be used for signal reconstruction as shown in Fig. 1. Hypercomplex Polar Fourier Descriptor (HPFD) is proposed as rotation invariant feature that can be used to represent image visual patterns. HPFD is not scale invariant comparing to [9]. Due to non commutative property of hypercomplex multiplication, both left-side and right-side hypercomplex polar Fourier analysis are studied. The proposed method treats image in a holistic manner and visual patterns are directly extracted from color images. To demonstrate the usefulness of proposed method as image analysis tool, experiments like image reconstruction, color plate test and image database retrieval are designed.

The organization of this paper is as follows. The basic theories of polar Fourier analysis, quaternion number and hypercomplex Fourier transform including mathematics descriptions are provided in Sect. 2. The proposed hypercomplex polar Fourier analysis with its properties are presented in Sect. 3. In Sect. 4, three experiments are designed to demonstrate the properties of the proposed method. The experimental results illustrate the effectiveness of our proposed method. Finally, Sect. 5 concludes this study.

2. Background

In this section, introductions about polar Fourier analysis, hypercomplex number and hypercomplex Fourier transform are given.

Manuscript received December 20, 2010.
Manuscript revised March 10, 2011.

[†]The authors are with the Graduate School of Information, Production and Systems, Waseda University, Kitakyushu-shi, 808–0135 Japan.
a) E-mail: joel@ruri.waseda.jp
b) E-mail: kam@waseda.jp

DOI: 10.1587/transinf.E94.D.1663

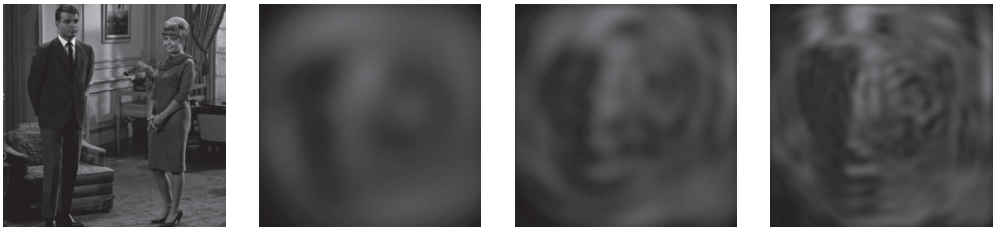

(a) Original Image (b) $n = 5$ (c) $n = 10$ (d) $n = 20$

(e) $n = 40$ (f) $n = 60$ (g) $n = 80$ (h) $n = 100$

Fig. 1 Image reconstruction using hypercomplex polar Fourier analysis.

2.1 Polar Fourier Analysis

Given a 2D image function $f(x, y)$, it can be transformed from cartesian coordinates to polar coordinates $f(r, \varphi)$, where r and φ denote radius and azimuth respectively. It is defined on the unit circle that $r \leq 1$, and can be expanded with respect to the basis functions $\Psi_{nm}(r, \varphi)$ as

$$f(r, \varphi) = \sum_{n=1}^{\infty} \sum_{m=-\infty}^{\infty} P_{nm} \Psi_{nm}(r, \varphi), \tag{1}$$

where the coefficient is

$$P_{nm} = \int_0^1 \int_0^{2\pi} f(r, \varphi) \Psi_{nm}^*(r, \varphi) r dr d\varphi. \tag{2}$$

The basis function is given by

$$\Psi_{nm}(r, \varphi) = R_{nm}(r) \Phi_m(\varphi), \tag{3}$$

where

$$R_{nm}(r) = \frac{1}{\sqrt{N_n^{(m)}}} J_m(x_{mn} r), \tag{4}$$

in which J_m is the m-th order first class Bessel series [16], and

$$\Phi_m(\varphi) = \frac{1}{\sqrt{2\pi}} e^{im\varphi}. \tag{5}$$

$N_n^{(m)}$ can be deduced by imposing boundary conditions according to the Sturm-Lioville (S-L) theory [18]. Two boundary conditions are interesting. With zero-value boundary condition,

$$N_n^{(m)} = \frac{1}{2} J_{m+1}^2(x_{mn}), \tag{6}$$

in which x_{mn} is the nth positive root for $J_m(x)$. With derivative boundary condition,

$$N_n^{(m)} = \frac{1}{2} \left(1 - \frac{m^2}{x_{mn}^2}\right) J_m^2(x_{mn}), \tag{7}$$

in which x_{mn} is the nth positive root for $J'_m(x)$.

Rewrite (2) with (3)–(7),

$$P_{nm} = \frac{1}{\sqrt{2\pi}} \int_0^1 \int_0^{2\pi} f(r, \varphi) R_{nm}(r) e^{-im\varphi} r dr d\varphi. \tag{8}$$

$|P_{nm}|$ is rotation invariant and is called Polar Fourier Descriptors (PFD). P_{nm} is complex number and its real part is

$$Re(P_{nm}) = \frac{1}{\sqrt{2\pi}} \int_0^1 \int_0^{2\pi} f(r, \varphi) R_{nm}(r) \cos(m\varphi) r dr d\varphi, \tag{9}$$

and its imaginary part is

$$Im(P_{nm}) = \frac{1}{\sqrt{2\pi}} \int_0^1 \int_0^{2\pi} f(r, \varphi) R_{nm}(r) \sin(-m\varphi) r dr d\varphi, \tag{10}$$

these two equations are used to deduce the relationship between Hypercomplex polar Fourier descriptor and conventional PFD as shown in Sect. 3.4. By using mathematical properties of trigonometric functions and associated Legendre polynomials, fast algorithms [17] are proposed to compute P_{nm} efficiently from digital images. Its computation time is one eighth of traditional one [10].

2.2 Quaternion Number

As a type of hypercomplex number and generalization of complex number, the quaternion was formally discusses by Hamilton in 1843 [2]. Its properties and applications have been studied [19]. Complex number has two components,

the real part and imaginary part. Quaternion has one real part and three imaginary parts. Given $a, b, c, d \in \mathbb{R}$, a quaternion $q \in \mathbb{H}$ ($\mathbb{H}$ denotes Hamilton) is defined as

$$q = \mathcal{S}(q) + \mathcal{V}(q), \mathcal{S}(q) = a, \mathcal{V}(q) = bi + cj + dk \quad (11)$$

where $\mathcal{S}(q)$ is scalar part and $\mathcal{V}(q)$ is vector part. i, j, k are imaginary operators obeying the following rules

$$\begin{aligned} &i^2 = j^2 = k^2 = -1, ij = -ji = k, \\ &jk = -kj = i, ki = -ik = j, \end{aligned} \quad (12)$$

From Eq. (12), the multiplication rule of quaternions is not commutative. The conjugate of a quaternion q is

$$\overline{q} = \mathcal{S}(q) - \mathcal{V}(q) = a - bi - cj - dk. \quad (13)$$

The norm of quaternion q is

$$\|q\| = \sqrt{a^2 + b^2 + c^2 + d^2}. \quad (14)$$

Quaternion q is named as unit quaternion if it is in set

$$\mathbb{U} = \{q | q \in \mathbb{H}, \|q\| = 1\}. \quad (15)$$

If quaternion q in following set,

$$\mathbb{P} = \{q | q \in \mathbb{H}, \mathcal{S}(q) = 0\}, \quad (16)$$

it is called pure quaternion. The quaternions belonging to set

$$\mathbb{S} = \{q | q \in \mathbb{U}, q \in \mathbb{P}\}, \quad (17)$$

are called unit pure quaternion. For two quaternions p and q, following rule holds

$$\overline{p \cdot q} = \overline{q} \cdot \overline{p}. \quad (18)$$

Euler formula holds for hypercomplex numbers,

$$e^{\mu\phi} = \cos(\phi) + \mu \sin(\phi) \quad (19)$$

We also have: $\|e^{\mu\phi}\| = 1$. The quaternion q can be represented in polar form: $q = \|q\| e^{\mu\phi}$.

Color image can be represented in pure quaternion form [4]

$$f(x, y) = f_R(x, y)i + f_G(x, y)j + f_B(x, y)k, \quad (20)$$

where $f_R(x, y)$, $f_G(x, y)$ and $f_B(x, y)$ are the red, green and blue components of the pixel, respectively.

2.3 Hypercomplex Fourier Transform

As the generalization of traditional Fourier transform, hypercomplex Fourier transform, its extensions and applications are studied [3]–[8]. Because of the noncommutative property of quaternion multiplication, three definitions for quaternion Fourier transform (QFT) are defined. The QFTs are defined by placing the integral kernels on the left side, right side and two sides of a quaternion function $f(x, y)$. Left-side QFT is defined as,

$$\boldsymbol{F}^{(l)}(\omega, \nu) = \int_{-\infty}^{\infty} \int_{-\infty}^{\infty} e^{-\mu_1(\omega x + \nu y)} f(x, y) dx dy, \quad (21)$$

right-side QFT is defined as,

$$\boldsymbol{F}^{(r)}(\omega, \nu) = \int_{-\infty}^{\infty} \int_{-\infty}^{\infty} f(x, y) e^{-\mu_1(\omega x + \nu y)} dx dy, \quad (22)$$

two-sides QFT is defined as,

$$\boldsymbol{F}^{(t)}(\omega, \nu) = \int_{-\infty}^{\infty} \int_{-\infty}^{\infty} e^{-\mu_1 \omega x} f(x, y) e^{-\mu_2 \nu y} dx dy, \quad (23)$$

where μ_1 and μ_2 are two unit pure quaternions that are orthogonal. Their relationships are studied [6].

3. Hypercomplex Polar Fourier Analysis and Its Properties

Inspired by Hypercomplex Fourier transform, we propose Hypercomplex Polar Fourier analysis. By introducing hypercomplex number to polar Fourier analysis, we define the transform function in Sect. 3.1. Its rotation invariance property is introduced in Sect. 3.2. In Sect. 3.3 relationship between right-side hypercomplex polar Fourier analysis and left-side hypercomplex polar Fourier analysis is established. Expansion of hypercomplex Polar Fourier analysis and its relationship with conventional Polar Fourier analysis are discussed in Sect. 3.4.

3.1 Hypercomplex Polar Fourier Descriptor

Given a 2D function $f(x, y)$, it can be transformed from cartesian coordinate to polar coordinate $f(r, \varphi)$, where r and φ denote radius and azimuth respectively. The following equations transform from cartesian coordinate to polar coordinate,

$$r = \sqrt{x^2 + y^2}, \quad (24)$$

and

$$\varphi = \arctan \frac{y}{x}. \quad (25)$$

Hypercomplex Polar Fourier analysis involves points within the largest inner circle of the image. After normalization, it is defined on the unit circle that $r \leq 1$ and can be expanded with respect to the basis function. Due to the noncommutative property of quaternion multiplication, here we define left-side Hypercomplex Polar Fourier analysis and right-side Hypercomplex Polar Fourier analysis.

Left-side Hypercomplex Polar Fourier analysis is defined as

$$f(r, \varphi) = \sum_{n=1}^{\infty} \sum_{m=-\infty}^{\infty} R_{nm}(r) e^{\mu m \varphi} HP_{nm}^{(l)}, \quad (26)$$

where the coefficient is

$$\begin{aligned} &HP_{nm}^{(l)}[f(r, \varphi); \mu] \\ &\quad = \frac{1}{\sqrt{2\pi}} \int_0^1 \int_0^{2\pi} R_{nm}(r) e^{-\mu m \varphi} f(r, \varphi) r dr d\varphi, \end{aligned} \quad (27)$$

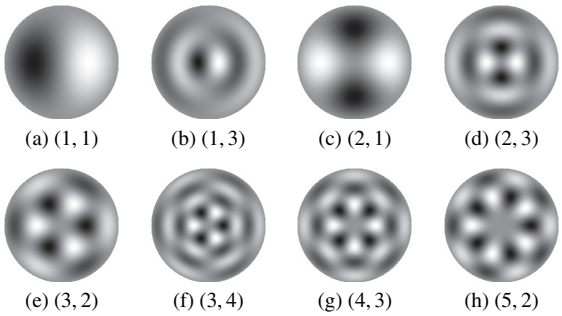

(a) (1, 1) (b) (1, 3) (c) (2, 1) (d) (2, 3)

(e) (3, 2) (f) (3, 4) (g) (4, 3) (h) (5, 2)

Fig. 2 Basic functions of HPFD.

where μ is unit pure quaternion and is defined as $\mu = \frac{1}{\sqrt{3}}i + \frac{1}{\sqrt{3}}j + \frac{1}{\sqrt{3}}k$.

Right-side hypercomplex polar Fourier analysis is defined as

$$f(r,\varphi) = \sum_{n=1}^{\infty}\sum_{m=-\infty}^{\infty} HP_{nm}^{(r)} R_{nm}(r) e^{\mu m\varphi}, \tag{28}$$

where the coefficient is

$$HP_{nm}^{(r)}[f(r,\varphi);\mu] = \frac{1}{\sqrt{2\pi}}\int_0^1\int_0^{2\pi} R_{nm}(r) f(r,\varphi) e^{-\mu m\varphi} r dr d\varphi. \tag{29}$$

The basis functions with different m, n values are shown in Fig. 2. Both left-hand hypercomplex polar Fourier analysis and right-hand hypercomplex polar Fourier analysis are reversible. Figure 1 shown that by using $HP_{nm}^{(r)}$, image can be reconstructed. With n increases bigger, more detail part of the image can be reconstructed.

3.2 Rotation Invariance

Given an image $f(r,\varphi)$, after rotated by an angle α the image is $f(r,\varphi+\alpha)$. We have

$$\begin{aligned} HP_{nm}^{\alpha} &= \frac{1}{\sqrt{2\pi}}\int_0^1\int_0^{2\pi} R_{nm}(r) e^{-\mu m(\varphi+\alpha)} f(r,\varphi+\alpha) r dr d\varphi \\ &= e^{-\mu m\alpha}\frac{1}{\sqrt{2\pi}}\int_0^1\int_0^{2\pi} R_{nm}(r) e^{-\mu m\varphi} f(r,\varphi) r dr d\varphi \\ &= e^{-\mu m\alpha} HP_{nm}. \end{aligned} \tag{30}$$

After applying norm operation, we have

$$\begin{aligned} \|HP_{nm}^{\alpha}\| &= \|e^{-\mu m\alpha} HP_{nm}\| \\ &= \|e^{-\mu m\alpha}\| \cdot \|HP_{nm}\| = \|HP_{nm}\|. \end{aligned} \tag{31}$$

As shown in Eq. (31), $\|HP_{nm}\|$ is rotation invariant and is named as Hypercomplex Polar Fourier Descriptor (HPFD). HPFD can be used to represent visual patterns. As hypercomplex polar Fourier analysis uses hypercomplex number representation, HPFD can directly represent patterns from color image.

3.3 Relationship between Right-Side and Left-Side Hypercomplex Polar Fourier Analysis

In this subsection, we discuss about the relationship between right-side hypercomplex polar Fourier analysis coefficient $HP_{nm}^{(r)}$ and left-side one $HP_{nm}^{(l)}$. Following the conjugate quaternion multiplication rule as shown in Eq. (18), conjugate operation is applied to $HP_{nm}^{(r)}$,

$$\begin{aligned} &HP_{nm}^{(r)}[f(r,\varphi);\mu] \\ &= \frac{1}{\sqrt{2\pi}}\int_0^1\int_0^{2\pi} R_{nm}(r) f(r,\varphi) e^{-\mu m\varphi} r dr d\varphi \\ &= \frac{1}{\sqrt{2\pi}}\overline{\int_0^1\int_0^{2\pi} R_{nm}(r)\overline{e^{-\mu m\varphi}}\cdot\overline{f(r,\varphi)} r dr d\varphi} \\ &= \frac{1}{\sqrt{2\pi}}\overline{\int_0^1\int_0^{2\pi} R_{nm}(r) e^{\mu m\varphi}\cdot\overline{f(r,\varphi)} r dr d\varphi} \\ &= \overline{HP_{nm}^{(l)}[\overline{f(r,\varphi)};-\mu]} \end{aligned} \tag{32}$$

Equation (32) shows that we can get right-side hypercomplex polar Fourier analysis from left-side one. They have equivalent effect on describing image patterns. In this paper, we use right-side one and denoted as HP_{nm}.

3.4 Expansion of HP_{nm}

In this subsection, we discuss about the expansion of hypercomplex polar Fourier analysis coefficient and its relationship with conventional polar Fourier analysis coefficient. By substitute Eqs. (9), (10), (19), and (20), we have

$$\begin{aligned} &HP_{nm} \\ &= \frac{1}{\sqrt{2\pi}}\int_0^1\int_0^{2\pi} R_{nm}(r) f(r,\varphi) e^{-\mu m\varphi} r dr d\varphi \\ &= \frac{1}{\sqrt{2\pi}}\int_0^1\int_0^{2\pi} R_{nm}(r)(f_R i + f_G j + f_B k) \\ &\qquad (\cos(-m\varphi) + \mu\sin(-m\varphi)) r dr d\varphi \\ &= i(Re(P_{nm}(f_R)) + \mu Im(P_{nm}(f_R))) \\ &\quad + j(Re(P_{nm}(f_G)) + \mu Im(P_{nm}(f_G))) \\ &\quad + k(Re(P_{nm}(f_r)) + \mu Im(P_{nm}(f_B))) \\ &= -\frac{1}{\sqrt{3}}(Im(P_{nm}(f_R)) + Im(P_{nm}(f_G)) + Im(P_{nm}(f_B))) \\ &\quad + \left\{Re(P_{nm}(f_R)) + \frac{1}{\sqrt{3}}[Im(P_{nm}(f_G)) - Im(P_{nm}(f_B))]\right\} i \\ &\quad + \left\{Re(P_{nm}(f_G)) + \frac{1}{\sqrt{3}}[Im(P_{nm}(f_B)) - Im(P_{nm}(f_R))]\right\} j \\ &\quad + \left\{Re(P_{nm}(f_B)) + \frac{1}{\sqrt{3}}[Im(P_{nm}(f_R)) - Im(P_{nm}(f_G))]\right\} k \end{aligned} \tag{33}$$

Equation (33) shows that the relationship between hypercomplex polar Fourier analysis coefficent and conventional

one. Rather than single channel analysis, the proposed method works in a holistic manner and directly extracts visual patterns from color images.

4. Experimental Results

Three experiments are given to demonstrate the usefulness of the proposed method as a image analysis tool. The first experiment is to test the rotation invariance of HPFD. The second experiment is color plate test. The last experiment is color image retrieval with HPFD.

Images with different content are tested to illustrate the effectiveness and feasibility of the proposed method. PC environment (Xeon 2.6 GHz, 2 G Memory) is used to perform these experiments. Following quaternion computation rules [20], algorithms are implemented by C++ and complied by gcc 4.3.2 on Linux 2.6.26. GNU Scientific Library [21] is used to calculate Bessel function and associated Legendre polynomials.

4.1 Rotation Invariance Evaluation

The objective of this experiment is to evaluate the rotation invariance property of HPFD. Eight standard images are used for this experiment as shown in Fig. 3. All the images are 256×256 pixels. As discussed in Eq. (31), magnitude of HPFD denoted as $\|HP_{nm}\|$ is invariant under rotation. To verify this property, relative error

$$\eta_{nm} = \left| \frac{\|HP_{nm}\| - \|HP^{\alpha}_{nm}\|}{\|HP_{nm}\|} \right|, \tag{34}$$

is calculated. The smaller the relative error is, the better it works under rotation.

As shown in Table 1, HPFD holds good invariance property under rotation. PFDs of the R, G, B images are calculated and integrated by average. The results are shown in Table 2. From the tables we can observe that mean value and standard deviation of HPFD relative error is smaller than that of PFD relative error. This experiment shows the rotation invariance property of HPFD and demonstrates that processing color image in a holistic way is robust.

4.2 Color Plate

In this experiment, the purpose is to compare the proposed HPFD and PFD for color plate test. As shown in Fig. 4 color plate images were used for color blind test. Figures 4 (a)–(d) are different images in color space. We can observe that they represent 1, 2, 3 and 4 respectively. Unfortunately they share same gray level image as shown in Fig. 4 (e). Both HPFD $\{HP_{mn}|m = 1,2,3,4,5, n = 1,2,3,4,5\}$ and PFD $\{P_{mn}|m = 1,2,3,4,5, n = 1,2,3,4,5\}$ are extracted for these four images. Features are extracted and compared with each other by normalized cross correlation,

$$ncc(P_m, P) = \left\langle \frac{P_m}{\|P_m\|}, \frac{P}{\|P\|} \right\rangle, \tag{35}$$

where $\langle \cdot, \cdot \rangle$ is the inner product, $\| \cdot \|$ is the L^2 norm and P_m is the features of match image.

As shown in Table 3 PFD failed to classify these four images. HPFD that process color image in a holistic way can successfully discriminate color images as demonstrated in Table 4.

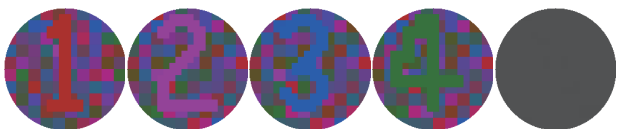

(a) (b) (c) (d) (e)

Fig. 4 Color plate images.

(a) (b) (c) (d)

(e) (f) (g) (h)

Fig. 3 Standard images for rotation invariance.

Table 1 Relative error of HPFD under rotation.

Image	η_{11}	η_{12}	η_{13}	η_{21}	η_{22}	η_{23}	η_{31}	η_{32}	η_{33}	Mean	Stdev
a	0.016	0.014	0.091	0.015	0.011	0.180	0.040	0.047	0.048	0.027	0.036
b	0.014	0.004	0.016	0.003	0.007	0.002	0.026	0.048	0.010	0.024	0.033
c	0.012	0.046	0.020	0.001	0.022	0.011	0.010	0.034	0.021	0.015	0.011
d	0.007	0.001	0.002	0.007	0.001	0.023	0.012	0.005	0.060	0.025	0.037
e	0.035	0.052	0.055	0.001	0.007	0.045	0.041	0.009	0.021	0.026	0.035
f	0.006	0.013	0.040	0.019	0.009	0.008	0.016	0.176	0.007	0.029	0.040
g	0.004	0.004	0.003	0.014	0.021	0.032	0.011	0.012	0.032	0.022	0.030
h	0.005	0.002	0.010	0.002	0.003	0.023	0.019	0.015	0.004	0.020	0.028

Table 2 Relative error of PFD under rotation.

Image	η_{11}	η_{12}	η_{13}	η_{21}	η_{22}	η_{23}	η_{31}	η_{32}	η_{33}	Mean	Stdev
a	0.032	0.014	0.105	0.017	0.024	0.182	0.108	0.052	0.049	0.033	0.039
b	0.012	0.010	0.064	0.004	0.007	0.001	0.027	0.037	0.017	0.035	0.051
c	0.013	0.039	0.021	0.003	0.025	0.012	0.010	0.035	0.019	0.018	0.011
d	0.011	0.006	0.003	0.027	0.009	0.024	0.024	0.019	0.064	0.038	0.058
e	0.041	0.052	0.075	0.003	0.015	0.053	0.071	0.009	0.047	0.038	0.054
f	0.005	0.041	0.042	0.055	0.009	0.006	0.096	0.353	0.009	0.042	0.064
g	0.004	0.029	0.003	0.015	0.023	0.062	0.015	0.016	0.031	0.033	0.046
h	0.017	0.023	0.009	0.016	0.042	0.021	0.061	0.016	0.023	0.031	0.043

Table 3 Similarity by PFD.

	a	b	c	d
a	1.000	1.000	1.000	1.000
b	1.000	1.000	1.000	1.000
c	1.000	1.000	1.000	1.000
d	1.000	1.000	1.000	1.000

Table 4 Similarity by HPFD.

	a	b	c	d
a	1.000	0.451	0.122	0.000
b	0.451	1.000	0.492	0.000
c	0.122	0.492	1.000	0.220
d	0.000	0.000	0.220	1.000

4.3 Color Image Retrieval

This experiment is designed to demonstrate effectiveness of the proposed method HPFD for color image retrieval. Content based image retrieval uses visual patterns to analyze actual content of images. Local binary pattern (LBP) treats images as local visual textures. By applying uniform operation LBP achieves rotation invariance [23]. Coordinated clusters representation (CCR) extracts spatial correlation between pixel intensities using the distribution function of the occurrence of texture units [24]. CCR and LBP work on gray image. Valuable information are lost by treating color image as gray level. Extending CCR to color image by color quantization, multilayer coordinated clusters representation (ML-CCR) has better retrieval result [25].

In this experiment we use Outex image database [22] that same as [25] (see Fig. 5). Outex image database is taken by rotating hardware device by following angles 0°, 5°, 10°, 15°, 30°, 45°, 60°, 75°, 90°. To search image database, proposed retrieval algorithm works as following steps

1. For the images $\{f_i(x, y)|i = 1, 2, \ldots\}$ in database, every image is processed one by one;
2. Given an image, interest points $\{I_i|i = 1, 2, \ldots, T\}$ are extracted by interest points detector [26], where T is total number of the interest points;
3. For image patch that is near interest point I_i within radius R, hypercomplex polar Fourier descriptor $|HP_{nm}|$ is extracted, in our experiment 25 features ($m = 1, 2, 3, 4, 5$ and $n = 1, 2, 3, 4, 5$) are computed;
4. Normalized cross correlation as shown in Eq. (35) is used to compare similarity of different image patches when retrieve the images. If the *ncc* is larger than predefined threshold τ. It is treated as matched image patch;
5. Similarity between two images depends on the number of total interest points T and the number of matched ones M;
$$sim(f_i(x, y), f_j(x, y)) = \frac{M}{T}, \tag{36}$$
6. The retrieved images are ordered by the similarity value $sim(\cdot, \cdot)$.

The detail experimental results are shown in Table 5. From the result we can observe that CCR and LBP work in gray image. CCR performs worse than LBP with uniform operation. ML-CCR works better than CCR after color quantization. Proposed image retrieval algorithm has promising accuracy. By treating color image in a holistic manner, proposed HPFD is effective for color textures and performs better than PFD. In RGB color space proposed algorithm using HPFD achieves best retrieval rate. This experiment testifies the effectiveness of the proposed method for color image retrieval.

5. Conclusions

In this paper, Hypercomplex Polar Fourier Analysis theory is proposed and its applications are studied. Inspired

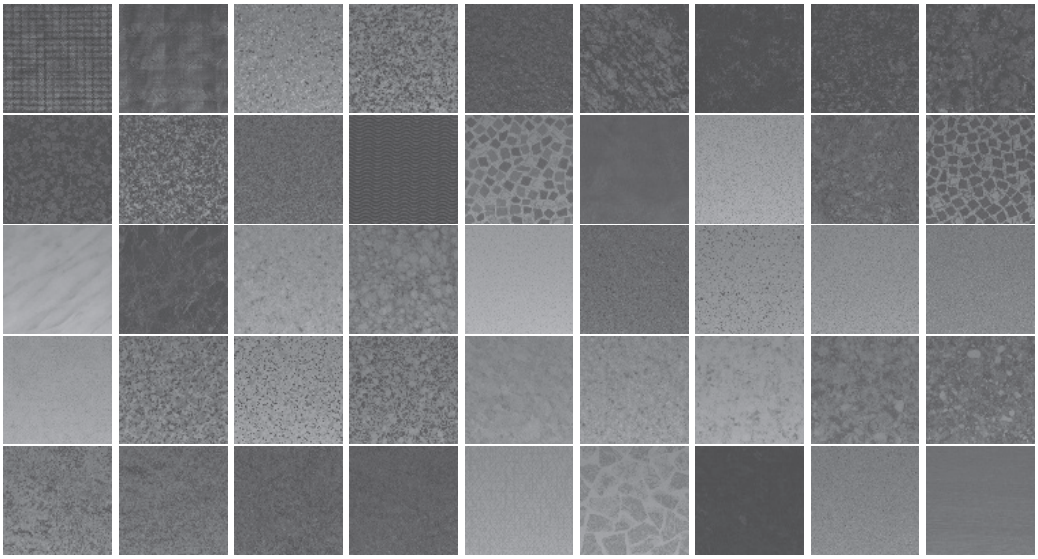

Fig. 5 Outex color image database.

Table 5 Outex Image database retrieval.

Feature	Color Space	Mean	0°	5°	10°	15°	30°	45°	60°	75°	90°
LBP	Gray	0.705	0.706	0.707	0.687	0.699	0.713	0.711	0.713	0.720	0.684
CCR	Gray	0.571	0.570	0.557	0.548	0.569	0.561	0.587	0.572	0.582	0.586
PFD	Gray	0.902	0.915	0.924	0.928	0.915	0.897	0.893	0.888	0.875	0.880
ML-CCR	RGB	0.848	0.863	0.860	0.842	0.833	0.855	0.840	0.857	0.854	0.827
ML-CCR	HSV	0.880	0.892	0.887	0.892	0.882	0.898	0.880	0.878	0.866	0.846
HPFD	RGB	0.929	0.933	0.946	0.937	0.946	0.933	0.915	0.924	0.911	0.920

by hypercomplex Fourier transform, hypercomplex number theory is introduced to polar Fourier analysis. By treating image in a holistic manner, hypercomplex polar Fourier analysis and mathematical properties are discussed. Hypercomplex Polar Fourier Descriptor that holds rotation invariance property is proposed. The relationship between left-side and right-side Hypercomplex polar Fourier analysis is established. By expanding the hypercomplex polar Fourier analysis coefficient, the relationship between the proposed one and conventional one has been found. Extensive experiments like image reconstruction, rotation invariance evaluation, color plate test and image database retrieval are designed to demonstrate the usefulness of the proposed method. Based on the experimental results, we can find that proposed method can extract valuable information from color images. Future works focus on extensions for spherical Fourier analysis and fast algorithms.

Acknowledgement

We would like to thank all people providing their image databases and science library for this study. This work was supported in part by Grant-in-Aid (No.21500181) for Scientific Research by the Ministry of Education, Science and Culture of Japan.

References

[1] R.N. Bracewell, The Fourier Transform and Its Applications, McGraw Hill, 2000.
[2] W.R. Hamilton, Elements of Quaternions, Longmans Green, London, New York, 1866.
[3] T.A. Ell, Hypercomplex Spectral Transforms, Ph.D. dissertation, Univ. Minnesota, Minneapolis, 1992.
[4] T.A. Ell and S.J. Sangwine, "Hypercomplex Fourier transforms of color images," IEEE Trans. Image Process., vol.16, no.1, pp.22–35, 2007.
[5] S.C. Pei, J.J. Ding, and J.H. Chang, "Efficient implementation of quaternion Fourier transform, convolution, and correlation by 2-D complex FFT," IEEE Trans. Signal Process., vol.49, no.11, pp.2783–2797, 2001.
[6] M.-H. Yeh, "Relationships among various 2-D quaternion Fourier transforms," IEEE Trans. Signal Process. Lett., vol.15, pp.669–672, 2008.
[7] S. Said, N. Le Bihan, and S.J. Sangwine, "Fast complexified quaternion Fourier transform," IEEE Trans. Signal Process., vol.56, no.4, pp.1522–1531, 2008.
[8] D.S. Alexiadis and G.D. Sergiadis, "Estimation of motions in color image sequences using hypercomplex Fourier transforms," IEEE Trans. Image Process., vol.18, no.1, pp.168–187, 2009.
[9] L.-Q. Guo and M. Zhu, "Quaternion Fourier-Mellin moments for color images," Pattern Recognit., vol.44, no.2, pp.187–195, 2011.
[10] Q. Wang, O. Ronneberger, and H. Burkhardt, "Rotational invariance based on Fourier analysis in polar and spherical coordinates," IEEE Trans. Pattern Anal. Mach. Intell., vol.31, no.9, pp.1715–1722, 2009.
[11] R. Bisseling and R. Kosloff, "The fast Hankel transform as a tool in

the solution of the time dependent Schringer equation," J. Computational Physics, vol.59, no.1, pp.136–151, 1985.
[12] D. Lemoine, "The discrete Bessel transform algorithm," J. Chemical Physics, vol.101, no.5, pp.3936–3944, 1994.
[13] K. Fu and E. Persoon, "Shape discrimination using Fourier descriptors," IEEE Trans. Pattern Anal. Mach. Intell., vol.8, no.3, pp.388–397, 1986.
[14] I. Bartolini, P. Ciaccia, and M. Patella, "Warp: Accurate retrieval of shapes using phase of Fourier descriptors and time warping distance," IEEE Trans. Pattern Anal. Mach. Intell., vol.27, no.1, pp.142–147, 2005.
[15] D. Zhang and G. Lu, "Shape-based image retrieval using generic Fourier descriptor," SP:IC, vol.17, no.10, pp.825–848, 2002.
[16] L. Andrews, Special Functions of Mathematics for Engineers, second ed., SPIE Press, 1997.
[17] Z. Yang and S. Kamata, "Fast polar and spherical Fourier descriptors for feature extraction," IEICE Trans. Inf. & Syst., vol.E93-D, no.7, pp.1708–1715, July 2010.
[18] W. Kosmala, Advanced Calculus: A Friendly Approach, Prentice-Hall, 1999.
[19] J.P. Ward, Quaternions and Cayley Numbers, Algebra and Applications, Kluwer, Norwell, MA, 1997.
[20] S. Sangwine and N. Le Bihan, "Quaternion toolbox for Matlab," http://qtfm.sourceforge.net/, 2005.
[21] The Gnu Scientific Library, http://www.gnu.org/software/gsl/, 2009.
[22] Outex Image database, http://www.outex.oulu.fi/index.php?page=image_acquisition, 2007.
[23] T. Ojala, M. Pietikainen, and T. Maenpaa, "Multiresolution gray-scale and rotation invariant texture classification with local binary patterns," IEEE Trans. Pattern Anal. Mach. Intell., vol.24, no.7, pp.971–987, 2002.
[24] E.V. Kurmyshev and R.E. Sanchez-Yanez, "Comparative experiment with colour texture classifiers using the CCR feature space," Pattern Recognit. Lett., vol.26, no.9, pp.1346–1353, 2005.
[25] F. Bianconi, A. Fernandez, E. Gonzalez, D. Caride and A. Calvino, "Rotation-invariant colour texture classification through multilayer CCR," Pattern Recognit. Lett., vol.30, no.8, pp.765–773, 2009.
[26] D.G. Lowe, "Distinctive image features from scale-invariant keypoints," Int. J. Comput. Vis., vol.60, no.2, pp.91–110, 2004.

Zhuo Yang received the B.E. and M.E. degree in control engineering and software engineering from Beijing Institute of Technology, Beijing, China, in 2005 and 2008 respectively. From 2006 to 2009 he worked in IBM China Development Lab. He is currently a Ph.D. student in Graduate School of Information, Production and Systems, Waseda University, Japan. His current research interests are mainly content based image retrieval and pattern recognition.

Sei-ichiro Kamata received the M.S. degree in computer science from Kyushu University, Fukuoka, Japan, in 1985, and the Doctor of Computer Science, Kyushu Institute of Technology, Kitakyushu, Japan, in 1995. From 1985 to 1988, he was with NEC, Ltd., Kawasaki, Japan. In 1988, he joined the faculty at Kyushu Institute of Technology. From 1996 to 2001, he has been an Associate Professor in the Department of Intelligent System, Graduate School of Information Science and Electrical Engineering, Kyushu University. Since 2003, he has been a professor in the Graduate School of Information, Production and Systems, Waseda University. In 1990 and 1994, he was a Visiting Researcher at the University of Maine, Orono. His research interests include image processing, pattern recognition, image compression, and space-filling curve application. Dr. Kamata is a member of the IEEE and the ITE in Japan.